Multiparticle Bose-Einstein correlations

Urs Achim Wiedemann

Institut für Theoretische Physik, Universität Regensburg, D-93040 Regensburg, Germany
Department of Physics, Columbia University, New York, New York 10027

Multiparticle symmetrization effects are contributions to the spectra of Bose-symmetrized states which are not the product of pairwise correlations. Usually they are neglected in particle interferometric calculations which aim at determining the geometry of the boson emitting source from the measured momentum distributions. Based on a method introduced by Zajc and Pratt, we give a calculation of all multiparticle symmetrization effects to the one- and two-particle momentum spectra for a Gaussian phase-space distribution of emission points. Our starting point is an ensemble of N-particle Bose-symmetrized wave functions with specified phase-space localization. In scenarios typical for relativistic heavy-ion collisions, multiparticle effects steepen the slope of the one-particle spectrum for realistic particle phase-space densities by up to 20 MeV, and they broaden the relative momentum dependence of the two-particle correlations. We discuss these modifications and their consequences in quantitative detail. Also, we explain how multiparticle effects modify the normalization of the two-particle correlator. The resulting normalization conserves event probabilities, which is not the case for the commonly used pair approximation. Finally, we propose a method of calculating Bose-Einstein weights from the output of event generators, taking multiparticle correlations into account.
[S0556-2813(98)01506-4]

PACS number(s): 25.75.Gz, 24.10.Cn, 52.60.+h

I. INTRODUCTION

Most hadrons are emitted in the final stage of a relativistic heavy-ion collision. They do not probe directly the hot and dense intermediate stages where quarks and gluons are expected to be the relevant physical degrees of freedom for equilibration processes. The geometrical size and dynamical state of the hadronic phase space emission region, however, depends sensitively on the entire evolution of the collision. This motivates current attempts to reconstruct its spatial and dynamical state from the experimental hadron spectra and to use it as a starting point for a dynamical back extrapolation into the hot and dense intermediate stages [1]. Two-particle correlations of identical particles which are sensitive to the space-time characteristics of the collision [2], play a crucial role in this approach. The reconstruction program based on their analysis has very good prospects: due to the increasing event multiplicities and larger statistics of the CERN SPS lead beam program (and the yet better quality data expected from the Relativistic Heavy Ion Collider RHIC at BNL), particle interferometric measurements start showing statistical errors on the few percent level. Also, systematic errors are increasingly better understood. Theoretical calculations should aim for a similar accuracy and control necessary approximations quantitatively.

One uncontrolled approximation used so far in almost all particle interferometric calculations is to neglect for the particle momentum spectra of Bose-Einstein symmetrized N-particle states all multiparticle correlations which cannot be written in terms of simpler pairwise ones. This reduces the number of $N!$ terms contributing to the two-particle correlator $C(\mathbf{K},\mathbf{q})$ to a manageable sum over all particle pairs. Beyond this approximation, two approaches have been used in the literature. First, Zajc has employed Monte Carlo techniques [3] to generate events with realistic multiparticle cor-

relations. This amounts to a shifting prescription $\{\mathbf{p}_i\} \rightarrow \{\mathbf{p}_i'\}$ which modifies the momentum distribution of simulated events according to unit weights (which themselves depend on the space-time structure of the source). Second, Zajc has found [3] the first steps towards a calculational scheme brought into final form by Pratt [4]: for model distributions, the N-particle spectra are given by a simple algorithm involving only two types of terms: C_m and G_m. In practice, this reduces the sums over all $N!$ permutations, typical for the calculation of momentum spectra, to sums over all partitions of N.

For both these approaches, there are first numerical calculations [3–5] and related analytical attempts [6–10] to control multiparticle effects to the one- and two-particle spectra, but a detailed study of their momentum dependence is missing, even for simple models. This work aims at filling this gap, making quantitative statements about the extent to which the slope of the one-particle spectrum and the relative momentum dependence of the two-particle correlations are modified due to multiparticle symmetrization effects. Our investigation takes the set Σ of phase-space emission points $(\mathbf{p}_i, \mathbf{r}_i, t_i)$ as *initial condition*. For notational simplicity, we restrict the discussion to one-particle species, like-charge pions say. To the set Σ, we associate a symmetrized N-particle wave function [11]

$$\Psi_N(\vec{\mathbf{X}},t) = \frac{1}{\sqrt{N!}} \sum_{s \in \mathcal{S}_N} \left(\prod_{i=1}^N f_{s_i}(\mathbf{X}_i,t) \right), \qquad (1.1)$$

where the sum runs over all permutations $s \in \mathcal{S}_N$ of the N indices, $\vec{\mathbf{X}}$ is a shorthand for the N three-dimensional coordinates $\mathbf{X}_i$, and the functions f_i denote single-particle wave packets centered around $(\mathbf{p}_i, \mathbf{r}_i)$ at initial time t_i and propagated according to the free time evolution. Final-state interactions, which imply a structure of the N-particle state dif-

ferent from Eq. (1.1), will not be considered in the present work. The wave function Ψ_N *defines* the boson emitting source. What we are interested in is the calculation of the one- and two-particle momentum spectra resulting from Eq. (1.1), the information they contain about the initial distribution of the "emission points" $z_i = (\mathbf{p}_i, \mathbf{r}_i, t_i)$, the extent to which these results modify the predictions of the pair approximation, and finally the algorithm which implements the numerical calculation of multiparticle spectra from the initial distribution Σ.

Our work is organized as follows: Section II shortly sets up and illustrates the general formalism via which particle momentum spectra are calculated from an N-particle state. In Sec. III, we discuss the properties of Gaussian wave packets which we choose for the single-particle states $f_i(\mathbf{X}_i, t)$ in Eq. (1.1). Section IV contains the main results. It gives a complete qualitative and quantitative analysis of multiparticle contributions to the one- and two-particle spectra for a boson emitting source of Gaussian phase-space distribution. In Sec. V, we discuss the implications of this model study for an algorithm which calculates the Hanbury-Brown–Twiss (HBT) radius parameters and momentum spectra for an arbitrary distribution of emission points. Results and related conceptual questions are summarized and discussed in the Conclusions.

II. THE FORMALISM

We want to determine for the N-particle symmetrized wave function Ψ_N the detection probability for measuring N identical bosons at time t at the positions $\mathbf{X}_i$ and momenta $\mathbf{P}_i$. We calculate first the N-particle Wigner phase-space density for Ψ_N [12]

$$
\begin{aligned}
\mathcal{W}_N(\vec{\mathbf{X}}, \vec{\mathbf{P}}, t) &= (2\pi)^{3N} \Psi_N(\vec{\mathbf{X}}, t) \\
&\times \left(\prod_{l=1}^{N} \delta^{(3)}(\mathbf{P}_l - \hat{\mathbf{P}}_l) \right) \Psi_N^*(\vec{\mathbf{X}}, t) \\
&= \frac{1}{N!} \sum_{s, s' \in \mathcal{S}_n} \prod_{l=1}^{N} W_{s'_l s_l}(\mathbf{X}_l, \mathbf{P}_l, t),
\end{aligned}
\tag{2.1a}
$$

$$
\begin{aligned}
W_{ij}(\mathbf{X}, \mathbf{P}, t) &= (2\pi)^3 f_i(\mathbf{X}, t) \delta^{(3)}(\mathbf{P} - \hat{\mathbf{P}}) f_j^*(\mathbf{X}, t) \\
&= \int d^3 \mathbf{y} \, e^{-i\mathbf{P}\cdot\mathbf{y}} f_i\left(\mathbf{X} + \frac{\mathbf{y}}{2}, t\right) f_j^*\left(\mathbf{X} - \frac{\mathbf{y}}{2}, t\right).
\end{aligned}
\tag{2.1b}
$$

Here, $\hat{\mathbf{P}}$ denotes the momentum operator acting on Ψ_N. The one-particle pseudo-Wigner functions $W_{ij}(\mathbf{X}, \mathbf{P}, t)$ provide the basic building blocks for the calculation of the N-particle momentum spectrum which is obtained by integrating Eq. (2.1a) over all spatial coordinates,

$$
\mathcal{P}_N(\vec{\mathbf{P}}) = \mathcal{N}_\psi \int d^3 \vec{\mathbf{X}} \mathcal{W}_N(\vec{\mathbf{X}}, \vec{\mathbf{P}}, t) = \frac{\mathcal{N}_\psi}{N!} \sum_{s, s' \in \mathcal{S}_n} \prod_{l=1}^{N} \mathcal{F}_{s'_l s_l}(\mathbf{P}_l),
\tag{2.2a}
$$

$$
\mathcal{F}_{ij}(\mathbf{P}) = \int d^3 \mathbf{X} W_{ij}(\mathbf{X}, \mathbf{P}) = D_i(\mathbf{P}) D_j^*(\mathbf{P}).
\tag{2.2b}
$$

where $\mathcal{N}_\psi$ is a normalization constant, $\mathcal{N}_\psi = 1/\langle \Psi_N | \Psi_N \rangle$, ensuring that the probability of detecting N particles is one. For a free time evolution of Ψ_N, the integration over the spatial components of Eq. (2.2a) leads to a time-independent expression $\mathcal{P}_N(\vec{\mathbf{P}})$, since interactions between the particles are necessary to change the momentum distribution in time. In contrast, integrating $\mathcal{W}_N(\vec{\mathbf{X}}, \vec{\mathbf{P}}, t)$ over all momenta leads to the detection probability of the N bosons at positions $\mathbf{X}_i$, which is a time-dependent quantity since free evolving bosons change their positions in time. The calculation of the N-particle momentum spectrum according to Eq. (2.2a) involves a sum over $(N!)^2$ terms. Due to the factorization of $\mathcal{F}_{ij}(\mathbf{P})$, this reduces to a sum over $N!$ terms,

$$
\mathcal{P}_N(\vec{\mathbf{P}}) = \frac{\mathcal{N}_\psi}{N!} \left| \sum_{s \in \mathcal{S}_n} \prod_{l=1}^{N} D_l(\mathbf{P}_{s(l)}) \right|^2.
\tag{2.3}
$$

In what follows, we are especially interested in the one- and two-particle momentum spectra $\mathcal{P}_N^1(\mathbf{P}_1)$, $\mathcal{P}_N^2(\mathbf{P}_1, \mathbf{P}_2)$ associated with the N-particle state Ψ_N. These are obtained by integrating $\mathcal{P}_N(\vec{\mathbf{P}})$ over all but one, respectively, two momenta,

$$
\mathcal{P}_N^1(\mathbf{P}_1) = \frac{\mathcal{N}_\psi}{N!} \sum_{s, s'} \mathcal{F}_{s'_1 s_1}(\mathbf{P}_1) \prod_{l=2}^{N} f_{s'_l s_l},
\tag{2.4a}
$$

$$
\mathcal{P}_N^2(\mathbf{P}_1, \mathbf{P}_2) = \frac{\mathcal{N}_\psi}{N!} \sum_{s, s'} \mathcal{F}_{s'_1 s_1}(\mathbf{P}_1) \mathcal{F}_{s'_2 s_2}(\mathbf{P}_2) \prod_{l=3}^{N} f_{s'_l s_l},
\tag{2.4b}
$$

$$
f_{ij} = \int d^3 \mathbf{P} \mathcal{F}_{ij}(\mathbf{P}).
\tag{2.4c}
$$

All particle momentum spectra are given in terms of the building blocks $D_i(\mathbf{P})$ (which determine $\mathcal{F}_{ij}$) and f_{ij}. Once the analytical form of the single-particle wave functions f_i is specified, these are readily calculated. In what follows, capital letters denote measurable position and momentum coordinates, small letters $\mathbf{p}_i$, $\mathbf{r}_i$, t_i denote the centers of wave packets which are not directly measurable. The only exception to this is the measurable relative momentum $\mathbf{q} = \mathbf{P}_1 - \mathbf{P}_2$ of the two-particle correlator $C[\mathbf{K} = \frac{1}{2}(\mathbf{P}_1 + \mathbf{P}_2), \mathbf{q}]$ which we denote by a small letter.

A. The Zajc-Pratt algorithm

Dynamical correlations between particles in the source are reflected in correlations in the set of emission points $(\mathbf{p}_i, \mathbf{r}_i, t_i)$. If there are no correlations, then the initial distribution of the centers of single-particle wave packets is given by a one-particle probability distribution $\rho(\mathbf{p}, \mathbf{r}, t)$. The n-particle spectra for a set of events with multiplicity N are then obtained by averaging over this distribution

$$
\bar{\mathcal{P}}_N^n(\mathbf{P}_1, \ldots, \mathbf{P}_n) = \int \left(\prod_{i=1}^{N} \mathcal{D}\rho_i \right) \mathcal{P}_N^n(\mathbf{P}_1, \ldots, \mathbf{P}_n),
\tag{2.5a}
$$

$$
\mathcal{D}\rho_i = d^3 \mathbf{r}_i d^3 \mathbf{p}_i dt_i \rho(\mathbf{p}_i, \mathbf{r}_i, t_i).
\tag{2.5b}
$$

A particular model distribution with correlations which assumes that the emission probability of a boson is increased if there is another emission in its vicinity [10], is obtained, e.g., by replacing in (2.5a)

$$\prod_{i=1}^{N} \rho(\mathbf{p}_i \mathbf{r}_i, t_i) \rightarrow \prod_{i=1}^{N} \rho(\mathbf{p}_i, \mathbf{r}_i, t_i) \frac{\langle \Psi_N | \Psi_N \rangle}{\omega(N)}. \qquad (2.6)$$

Here $\omega(N)$ is an averaged normalization defined below. The technical advantage of adopting (2.6) is that the $(\mathbf{p}_i, \mathbf{r}_i, t_i)$-dependent normalization factor $\mathcal{N}_\Psi$ in the spectrum $\mathcal{P}_N^n$ of (2.5a) is canceled. This allows us to write without approximation all spectra in terms of the building blocks [4]

$$G_m(\mathbf{P}_1, \mathbf{P}_2) = \int \left(\prod_{l=1}^{m} \mathcal{D}\rho_{i_l} \right) D_{i_1}^*(\mathbf{P}_1) f_{i_1 i_2} f_{i_2 i_3}$$
$$\times \cdots f_{i_{m-1} i_m} D_{i_m}(\mathbf{P}_2), \qquad (2.7a)$$

$$C_m = \int d^3 \mathbf{P} \, G_m(\mathbf{P}, \mathbf{P}). \qquad (2.7b)$$

The resulting Zajc-Pratt (ZP) algorithm for the calculation of one- and two-particle spectra reads [3,4,10]

$$w(N) = \sum_{(n,l_n)_N} \frac{N!}{\Pi_n n^{l_n}(l_n!)} C_1^{l_1} C_2^{l_2} \ldots C_n^{l_n}, \qquad (2.8)$$

$$\bar{\mathcal{P}}_N^1(\mathbf{P}) = \sum_{m=1}^{N} \frac{(N-1)!}{(N-m)!} \frac{w(N-m)}{\omega(N)} G_m(\mathbf{P}, \mathbf{P}), \qquad (2.9)$$

$$\bar{\mathcal{P}}_N^2(\mathbf{P_1}, \mathbf{P_2}) = \sum_{J=2}^{N} \frac{(N-2)!}{(N-J)!} \frac{w(N-J)}{\omega(N)}$$
$$\times \sum_{i=1}^{J-1} [G_i(\mathbf{P}_1, \mathbf{P}_1) G_{J-i}(\mathbf{P}_2, \mathbf{P}_2)$$
$$+ G_i(\mathbf{P}_1, \mathbf{P}_2) G_{J-i}(\mathbf{P}_2, \mathbf{P}_1)]. \qquad (2.10)$$

These spectra are normalized to unity. In Appendix A, we give their derivation in some combinatorical detail. Due to the ZP algorithm, the calculation of the N-particle spectra is reduced from sums over all permutations to sums over all partitions $(n, l_n)_N$ of a set of N points into l_n subsets of n points, $N = \Sigma_n l_n n$. The number of partitions of N grows asymptotically like $e^{\sqrt{N}}$. For explicit calculations with event multiplicities in the hundreds, it is hence important to get control over the m dependence of the Pratt terms C_m and G_m. This is our strategy in Sec. IV.

B. A simple example: the Zajc model

To illustrate the above formalism, we consider a normalized N-particle density matrix $\rho_\pi^{(N)}$ for multiparticle states $|\mathbf{x}_1, \ldots, \mathbf{x}_N\rangle$, created by repeated operation of the single-particle creation operator $\phi^\dagger(\mathbf{x})$,

$$\phi^\dagger(\mathbf{x}) = \int \frac{d^3\mathbf{k}}{(2\pi)^{3/2}} e^{i\mathbf{k}\cdot\mathbf{x}} g(\mathbf{k}) a_\mathbf{k}^\dagger, \qquad (2.11a)$$

$$\rho_\pi^{(N)} = \mathcal{N} \int d\mathbf{x}_1 \ldots d\mathbf{x}_N \rho(\mathbf{x}_1) \ldots \rho(\mathbf{x}_N)$$
$$\times |\mathbf{x}_1, \ldots, \mathbf{x}_N\rangle\langle \mathbf{x}_1, \ldots, \mathbf{x}_N|. \qquad (2.11b)$$

This density matrix specifies in particular the one- and two-particle spectra $\text{Tr}[\rho_\pi^{(n)} a_\mathbf{P}^\dagger a_\mathbf{P}]$ and $\text{Tr}[\rho_\pi^{(n)} a_{\mathbf{P}_1}^\dagger a_{\mathbf{P}_2}^\dagger a_{\mathbf{P}_1} a_{\mathbf{P}_2}]$. For the Gaussian model distribution [3]

$$\frac{|g(\mathbf{k})|^2}{(2\pi)^3} = (2\pi p_0^2)^{-3/2} \exp[-\mathbf{k}^2/2p_0^2], \qquad (2.12a)$$

$$\rho(\mathbf{x}) = (\pi R^2)^{-3/2} \exp[-\mathbf{x}^2/R^2], \qquad (2.12b)$$

the effects of multiparticle correlations on the HBT-radius parameters have been considered already by Zajc. His discussion however is restricted to an explicit calculation of three-particle symmetrization effects and to qualitative estimates of higher-order contributions. Here, we demonstrate that the ZP algorithm allows for a complete quantitative analysis of the Zajc model. The first step is to identify the building blocks of the particle spectra (2.4),

$$D_i(\mathbf{P}) = \frac{g(\mathbf{P})}{(2\pi)^{3/2}} \exp[i\mathbf{P}\cdot\mathbf{x}_i], \qquad (2.13a)$$

$$f_{ij} = \exp\left[-\frac{p_0^2}{2}(\mathbf{x}_i - \mathbf{x}_j)^2\right]. \qquad (2.13b)$$

The calculation of the terms C_m reduces then to m-dimensional Gaussian integrations. One finds $C_1 = 1$ and

$$C_m = (1 + p_0^2 R^2)^{-3(m-1)/2} \left(\frac{1-h}{\det B_m}\right)^{3/2}, \qquad (2.14a)$$

$$\det B_m = \frac{h^m}{2^{m-1}} \left(T_m\left(\frac{1}{h}\right) - 1\right), \qquad (2.14b)$$

$$h = \frac{1}{1 + 1/c}, \quad c = R^2 p_0^2,$$

where T_m denotes Chebysheff polynomials of the first kind [13]. The momentum-dependent terms read

$$G_m(\mathbf{K}, \mathbf{q}) = C_m \frac{(1 + g_K^{(m)})^{3/2}}{(2\pi p_0^2)^{3/2}} \exp[-\mathbf{K}^2 g_K^{(m)}/2p_0^2]$$
$$\times \exp[-(R^2 g_Q^{(m)}/4 + 1/8p_0^2)\mathbf{q}^2] \qquad (2.15a)$$

$$g_Q^{(m)} = \frac{1}{4} \vec{e}_+^{\,t} A_m^{-1} \vec{e}_+, \quad e_+^{(i)} = \delta_{i1} + \delta_{im}, \qquad (2.15b)$$

$$g_K^{(m)} = \frac{c}{2} \vec{e}_-^{\,t} A_m^{-1} \vec{e}_- + 1, \quad e_-^{(i)} = \delta_{i1} - \delta_{im}, \qquad (2.15c)$$

$$(A_m)_{ij} = (1 + c)\delta_{ij} - \frac{c}{2}(\delta_{i,j+1} + \delta_{i+1,j}). \qquad (2.15d)$$
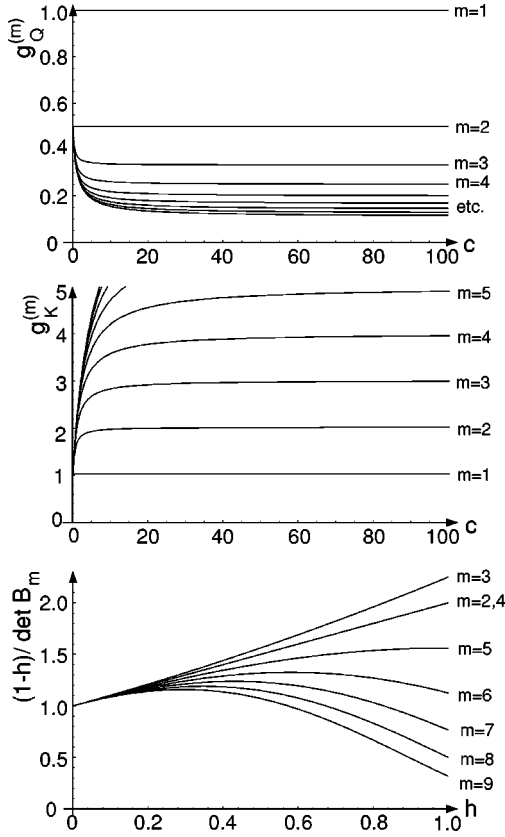
FIG. 1. The terms $g_Q^{(m)}$, $g_K^{(m)}$ and the remainder term $(1-h)/\mathrm{det}B_m$ characterize the $\mathbf{q}$ dependence, $\mathbf{K}$ dependence, and weight of Pratt terms and hence the momentum dependence of particle spectra. Their m dependence contains information about how higher-order multiparticle correlations affect the spectra. Results are shown for the Zajc model (2.12).

The main message of these involved but explicit expressions is contained in the m dependence of the terms $g_Q^{(m)}$ and $g_K^{(m)}$. These specify the $\mathbf{K}$ and $\mathbf{q}$ dependence of the building blocks G_m and hence of all spectra. Here, they are functions of the phase-space volume $V = p_0^3 R^3$ only, and their behavior can be understood by simple arguments:

The factors $g_K^{(m)}$ generically increase with increasing m, see Fig. 1. Especially, in a limiting case, one finds

$$\lim_{V \to \infty} g_K^{(m)} = m. \qquad (2.16)$$

The reason is that Bose-Einstein symmetrization effects enhance the low momentum region of the one-particle spectrum, leading to steeper slopes. This one-particle spectrum $\bar{\mathcal{P}}_N^1(\mathbf{P})$ is a linear superposition of Gaussian terms $G_m(\mathbf{K}, \mathbf{q} = 0)$, which due to $g_K^{(m)}$ show increasingly steeper slopes.

The $\mathbf{q}$ dependence of G_m governs the $\mathbf{q}$ dependence of the two-particle spectrum. The terms $g_Q^{(m)}$ depicted in Fig. 1 decrease with increasing m and have the limiting values

$$\lim_{V \to \infty} g_Q^{(m)} = \frac{1}{m}. \qquad (2.17)$$

Zajc has concluded on the basis of this behavior that [3] ''the two-particle correlation function becomes a superposition of terms with successively broader distribution in $\mathbf{P}_1 - \mathbf{P}_2$, leading to an increasingly smaller value for the inferred radius.'' The reason is that Bose-Einstein symmetrization effects enhance the probability of finding bosons closer together in configuration space and hence result in broader $\mathbf{q}$ distributions of the two-particle spectra.

The above arguments explain the effect of multiparticle correlations qualitatively. For a quantitative understanding, the weights of higher-order terms contributing to the one- and two-particle spectra are important. These weights are governed by the terms C_m which [up to a correction factor $(1-h)/\mathrm{det}B_m$ of order unity] essentially decrease like $(m-1)$th powers of the inverse phase space volume. For event multiplicities in the hundreds, a quantitative analysis can then be done numerically, using the analytical expressions (2.14) and (2.15). We defer such a study to a slightly more general model in Sec. IV where certain analytical simplifications allow for a more transparent discussion. A short comparison of the qualitative and quantitative properties of the models studied here and in Sec. IV is given in the text following Eq. (4.4).

III. GAUSSIAN WAVEPACKETS

In the example of Sec. II B, we have started from single-particle creation operators $\phi^\dagger$ whose momentum support $g(\mathbf{k})$ does not carry a label i. As a consequence, the N-particle states considered in Sec. II B are build up from N single-particle wave functions with *identical* phase-space localization. We now adopt a more general setting in which a set of N phase-space points $(\mathbf{p}_i, \mathbf{r}_i, t_i)$ is associated with N Gaussian wave packets f_i, centered at initial time t_i around the points $(\mathbf{p}_i, \mathbf{r}_i)$ with spatial width σ [14,15,11],

$$f_i(\mathbf{X}, t_i) = \frac{1}{(\pi \sigma^2)^{3/4}} \exp\left[-\frac{1}{2\sigma^2}(\mathbf{X} - \mathbf{r}_i)^2 + i\mathbf{p}_i \cdot \mathbf{X} \right]. \qquad (3.1)$$

The Fourier transform of f_i is proportional to $\exp[-\sigma^2(\mathbf{k} - \mathbf{p}_i)^2/2 - i\mathbf{r}_i \cdot (\mathbf{k} - \mathbf{p}_i)]$ and can be compared to the momentum support of $\phi^\dagger$ in Eq. (2.11a). The corresponding N-particle symmetrized states reduce to those considered in Sec. II B for $p_0 = 1/\sigma$ and $\mathbf{p}_i = 0 = \mathbf{r}_i$, when the momentum support function becomes independent of the particle label i.

The one-boson state (3.1) is optimally localized around $(\mathbf{p}_i, \mathbf{r}_i)$ in the sense that it saturates the Heisenberg uncertainty relation $\Delta \mathbf{x} \cdot \Delta \mathbf{p}_x = 1$, with $\Delta x_i = \sigma$ at initial time $t = t_i$. Different choices of single-particle wave functions can lead to different results for the calculated spectra. We have some control over the extent to which different choices matter by finally checking the σ dependence of our results. The model parameter can range between $\sigma \in [0, \infty]$. In Refs. [11] and [16], it was argued that a realistic value for σ is for pions of the order of the Compton wavelength.

The free time evolution of f_i is specified by the one-particle Hamiltonian H_0 which acts as a multiplication operator in momentum space,

$$f_{z_i}(\mathbf{X},t)=(e^{-iH_0(t-t_i)}f_i)(\mathbf{X},t)$$

$$=\frac{1}{(2\pi)^3}\int d^3k e^{i\mathbf{k}\cdot\mathbf{X}-iE_{\mathbf{k}}(t-t_i)}\tilde{f}_i(\mathbf{k}). \quad (3.2)$$

The resulting building blocks for the N-particle spectra are

$$D_i(\mathbf{P})=2^{3/2}(\pi\sigma^2)^{3/4}e^{-(\sigma^2/2)(\mathbf{p}_i-\mathbf{P})^2}e^{iE_Pt_i-i\mathbf{P}\cdot\mathbf{r}_i}, \quad (3.3a)$$

$$s_i(\mathbf{P})=\mathcal{F}_{ii}(\mathbf{P})=2^3(\pi\sigma^2)^{3/2}e^{-\sigma^2(\mathbf{p}_i-\mathbf{P})^2}. \quad (3.3b)$$

To streamline our notation, we have neglected in D_i a factor $\exp[i\mathbf{r}_i\cdot\mathbf{p}_i]$. The product of these factors cancels in the calculation of the Wigner function (2.1b) and *a fortiori* in all the functions derived from it. The function $s_i(\mathbf{P})=\mathcal{F}_{ii}(\mathbf{P})$ denotes the probability that a boson in the state f_i is detected with momentum $\mathbf{P}$. This measured momentum $\mathbf{P}$ has a Gaussian distribution around the central momentum $\mathbf{p}_i$ of the wave packet.

The functions f_{ij} in Eq. (2.4c) characterize the overlap between the wave packets f_i and f_j and play an important role in the ZP algorithm. They take a particularly simple form if all particles are emitted in a flash,

$$f_{ij}\propto\exp\left[-\frac{1}{4\sigma^2}(\mathbf{r}_i-\mathbf{r}_j)^2-\frac{\sigma^2}{4}(\mathbf{p}_i-\mathbf{p}_j)^2\right]$$

$$\times\exp\left[-\frac{i}{2}(\mathbf{p}_i+\mathbf{p}_j)\cdot(\mathbf{r}_i-\mathbf{r}_j)\right]. \quad (3.4)$$

All terms contributing to $\mathcal{P}_N^1$ or $\mathcal{P}_N^2$ contain the same number of factors f_{ij} and hence, the normalization of f_{ij} does not matter in what follows. For notational convenience, we change it by fixing $f_{ii}=1$. The functions f_{ij} measure the distance $|z_i-z_j|$ between the phase-space points i and j. This distance measure depends on the wave packet width σ but leaves the phase-space volume independent of σ,

$$|f_{ij}|=\exp[-\tfrac{1}{4}|z_i-z_j|^2], \quad (3.5)$$

$$z_j=\frac{1}{\sigma}r_j+i\sigma p_j.$$

IV. MULTIPARTICLE CORRELATIONS FOR A GAUSSIAN MODEL

We now determine quantitatively multiparticle correlation effects for a source of N identical bosons whose wave packets of spatial width σ are emitted instantaneously according to a Gaussian phase-space distribution (2.6) with

$$\rho(\mathbf{p},\mathbf{r})=\frac{\delta(t)}{\pi^3 R^3\Delta^3}\exp\left[-\frac{\mathbf{r}^2}{R^2}-\frac{\mathbf{p}^2}{\Delta^2}\right]. \quad (4.1)$$

Our main aim is to study for this model the extent to which multiparticle correlations modify the slope of the one-particle spectrum and the width of the two-particle correlator. To this end, we calculate first the building blocks of the ZP algorithm. Having explicit expressions for $g_Q^{(m)}$,

$g_K^{(m)}$, and C_m in terms of simple polynomials will simplify our discussion considerably. The corresponding first-order Pratt terms are

$$C_1=1, \quad (4.2a)$$

$$G_1(\mathbf{P}_1,\mathbf{P}_2)=(1+\sigma^2\Delta^2)^{-3/2}$$

$$\times\exp\left[-\left(\frac{\sigma^2}{4}+\frac{R^2}{4}\right)\mathbf{q}^2\right]$$

$$\times\exp\left[-\frac{1}{\Delta^2+1/\sigma^2}\mathbf{K}^2\right]. \quad (4.2b)$$

All higher-order Pratt terms can be calculated explicitly as averages over relative and average pair distributions. Details are given in Appendix B. The momentum-independent terms read

$$C_m=(h_1^{(m)}h_2^{(m)})^{-3/2}\left(\left[1+\frac{\sigma^2\Delta^2}{2}\right]\left[1+\frac{R^2}{2\sigma^2}\right]\right)^{-3(m-1)/2}, \quad (4.3a)$$

$$h_1^{(m)}=\sum_{k=0}^{m-1}\binom{m-1}{k}a^{k/2|^h}b^{k/2|^l}, \quad (4.3b)$$

$$h_2^{(m)}=\sum_{k=0}^{m-1}\binom{m-1}{k}a^{k/2|^l}b^{k/2|^h}, \quad (4.3c)$$

$$a=\frac{1}{1+2\sigma^2/R^2}, \quad b=\frac{1}{1+2/\sigma^2\Delta^2}. \quad (4.3d)$$

Here, $k/2|^l$ denotes the greatest integer not larger than $k/2$ (floor), and $k/2|^h$ the least integer not smaller than $k/2$ (ceiling). The notational shorthands a and b range between 0 and 1 depending on the phase-space localization of the wave packet centers, i.e., they map the whole parameter space $0<R<\infty$, $0<\Delta<\infty$ of the model (4.1) onto a finite region. The momentum-dependent terms are given by

$$G_m(\mathbf{P}_1,\mathbf{P}_2)=C_m\left(\frac{2\pi}{\Delta^2}bg_K^{(m)}\right)^{3/2}$$

$$\times\exp\left[-\left(\frac{\sigma^2}{4}+\frac{R^2}{8}\right)g_Q^{(m)}\mathbf{q}^2\right]$$

$$\times\exp\left[-\frac{2}{\Delta^2}bg_K^{(m)}\mathbf{K}^2\right], \quad (4.4a)$$

$$g_Q^{(m)}=h_3^{(m)}/h_2^{(m)}, \quad (4.4b)$$

$$g_K^{(m)}=h_1^{(m)}/h_3^{(m)}, \quad (4.4c)$$

$$h_3^{(m)}=1+\sum_{k=1}^{m}(ab)^k\binom{m}{2k}. \quad (4.4d)$$

The comparison of the present model calculation with the Zajc model (2.12) is not straightforward. As mentioned in

the sequel of Eq. (3.1), the wave packets used in both models can be compared by setting the wave packet centers $\mathbf{p}_i = 0 = \mathbf{r}_i$. However, the integral over $\rho(\mathbf{x})$ in Eq. (2.11b) performs an average over the positions $\mathbf{x}$, while in the model (4.1) we do not average over the position $\mathbf{X}$ but over the centers of wave packets $\mathbf{p}_i$, $\mathbf{r}_i$. Due to these different starting points, the Zajc model is not a simple limiting case of Eq. (4.1). Nevertheless, main features of the Zajc model (2.12) can be reproduced qualitatively in the present model. The leading contribution of the momentum-independent Pratt terms C_m shows again a power-law behavior. Also, the m dependence of the terms $g_Q^{(m)}$ and $g_K^{(m)}$ of the Zajc model is recovered in certain limiting cases,

$$\lim_{a \to 0 \atop b \to 1} g_Q^{(m)} = \frac{1}{m}, \tag{4.5a}$$

$$\lim_{a \to 1 \atop b \to 0} g_K^{(m)} = m. \tag{4.5b}$$

In general, however, the m dependence of the terms $g_Q^{(m)}$ and $g_K^{(m)}$ is much weaker in the present model. Especially, there is no limit in which both $g_Q^{(m)} = 1/m$ and $g_K^{(m)} = m$. These differences between both models may provide a first idea about the extent to which the choice of the model distribution affects our conclusions.

A. Weighting multiparticle contributions

The normalization $\omega(N)$ is not a direct physical observable, but it determines the weights with which multiparticle correlations contribute to the particle spectra. To see this, we consider the one-particle spectrum,

$$\bar{\mathcal{P}}_N^1(\mathbf{P}) = \sum_{m=1}^N v_m G_m(\mathbf{P}, \mathbf{P})/C_m. \tag{4.6}$$

The mth order contributions G_m/C_m are normalized to one, and the weights v_m add up to unity,

$$1 = \sum_{m=1}^N v_m, \tag{4.7a}$$

$$v_m = \frac{(N-1)!}{(N-m)!} \frac{\omega(N-m)}{\omega(N)} C_m. \tag{4.7b}$$

The lowest order contribution G_1/C_1, by which the one-particle spectrum is typically approximated, contributes a fraction v_1 only, the value $(1 - v_1)$ characterizes the importance of higher-order contributions. For a quantitative analysis we now determine the dependence of the normalization $\omega(N)$ and the weights v_m on the event multiplicity N and the phase space density of the emission region.

We consider the terms C_m, the building blocks of $\omega(N)$. For the present model, these are given in Eq. (4.3a). The factor $(h_1^{(m)} h_2^{(m)})$ in this equation ranges between 1 and $2^{2(m-1)}$, and can be written as

$$(h_1^{(m)} h_2^{(m)}) = f_{\text{corr}}^{(m)} (1 + \sqrt{ab})^{2(m-1)}, \tag{4.8a}$$

$$f_{\text{corr}}^{(m)} \in \left[\sqrt{\frac{a}{b}}, \sqrt{\frac{b}{a}} \right]. \tag{4.8b}$$

The correction factor $f_{\text{corr}}^{(m)}$ appears only linearly in the expressions for C_m, rather than as an mth power, and it is of order $O(1)$ (it is exactly $f_{\text{corr}}^{(m)} = 1$ for a choice of parameters R and Δ such that $a = b$). This allows for the approximation

$$C_m \simeq \epsilon^{m-1}, \tag{4.9a}$$

$$\epsilon(R, \Delta) = \left(\left[1 + \frac{\sigma^2 \Delta^2}{2} \right] \left[1 + \frac{R^2}{2\sigma^2} [1 + \sqrt{ab}]^2 \right] \right)^{-3/2}, \tag{4.9b}$$

with which the normalization $\omega(N)$ takes the simple form

$$\omega(N) = \sum_{k=1}^N S_N^{(k)} \epsilon^{(N-k)} = (-\epsilon)^N \frac{\Gamma(-1/\epsilon + 1)}{\Gamma(-1/\epsilon + 1 - N)}$$

$$= \prod_{k=1}^N [1 + \epsilon(k-1)]. \tag{4.10}$$

Here, the combinatorical factors $S_N^{(k)}$ denote the number of permutations of N elements which contain exactly k cycles. They are commonly referred to as Stirling numbers of the first kind. We have used their generating function in terms of Γ functions [17].

We can now determine the weights of multiparticle contributions to the one- and two-particle spectra. For the one-particle spectrum, we find by inserting Eq. (4.11) into the ZP algorithm

$$\rho_{\text{vol}} := N\epsilon, \tag{4.11a}$$

$$v_1 = \frac{1}{1 + \epsilon(N-1)} \approx \frac{1}{1 + \rho_{\text{vol}}}, \tag{4.11b}$$

$$v_m \approx \frac{\rho_{\text{vol}}^{m-1}}{(1 + \rho_{\text{vol}})^m}. \tag{4.11c}$$

The approximation in the last line is valid for large multiplicities, when $m \ll N$. Similarly, the weights u_m for the different contributions to the two-particle momentum spectrum can be calculated. Using the power-law behavior $C_m = \epsilon^{m-1}$, we find

$$\bar{\mathcal{P}}_N^2(\mathbf{P}_1,\mathbf{P}_2) = \sum_{m=2}^{N} u_m \sum_{i=1}^{m-1} H_{i,m-i}(\mathbf{P}_1,\mathbf{P}_2), \quad (4.12a)$$

$$H_{i,m-i}(\mathbf{P}_1,\mathbf{P}_2) = \frac{G_i(\mathbf{P}_1,\mathbf{P}_1)}{C_i} \frac{G_{m-i}(\mathbf{P}_2,\mathbf{P}_2)}{C_{m-i}}$$
$$+ \frac{G_i(\mathbf{P}_1,\mathbf{P}_2)}{C_i} \frac{G_{m-i}(\mathbf{P}_2,\mathbf{P}_1)}{C_{m-i}},$$
$$(4.12b)$$

where

$$u_m = \frac{(N-2)!}{(N-m)!} \frac{\omega(N-m)}{\omega(N)} \epsilon^{m-2} \approx \frac{\rho_{\mathrm{vol}}^{m-2}}{(1+\rho_{\mathrm{vol}})^m} = \frac{v_{m-1}}{(1+\rho_{\mathrm{vol}})}. \quad (4.13)$$

Again, the approximation in the last line is valid for large multiplicities, when $m \ll N$. To sum up: multiparticle correlations account for a fraction $\rho_{\mathrm{vol}}/(1+\rho_{\mathrm{vol}})$ of the one-particle spectrum. For the two-particle spectrum, they are somewhat more important: the pure pairwise correlations receive only a weight $1/(1+\rho_{\mathrm{vol}})^2$.

For sufficiently large event multiplicities, the weights v_m and u_m of multiparticle contributions are not separate functions of ϵ and N, but functions of the product ρ_{vol} only. The physics entering ρ_{vol} can be most easily illustrated in the large phase-space volume limit, when

$$\epsilon \approx \frac{1}{(R^3 \Delta^3)}, \quad \text{for } \frac{R}{\sigma}, \Delta \cdot \sigma \gg 1. \quad (4.14)$$

We hence call ρ_{vol} a "phase-space density of emission points." This notion should not be taken too literally: the product of the volumes of three-dimensional spheres in position and momentum space is $(4/3\,\pi)^2 R^3 \Delta^3$, and hence, ρ_{vol} is for large sources approximately a factor 10 larger than the particle number per unit phase-space cell. Also, for realistic source sizes, the value of ϵ deviates significantly from the approximation (4.14), and a calculation of ρ_{vol} starting from Eq. (4.9b) is preferable.

One can ask whether in the large-N limit, the normalization $\omega(N)$ becomes a function of ρ_{vol} only. To clarify this, we recall that a product $\Pi_{k=1}^{N}(1+a_k)$ with $a_k \geq 0$ has a $N \rightarrow \infty$-limit if and only if $\Sigma_{k=1}^{\infty} a_k$ converges. For the normalization (4.10), we find $\Sigma_{k=1}^{N} a_k = \frac{1}{2}\epsilon N(N-1)$, i.e., for fixed phase-space density,

$$\lim_{N \rightarrow \infty} \omega(N)\big|_{\rho_{\mathrm{vol}}=\mathrm{fixed}} \rightarrow \infty. \quad (4.15)$$

There is no physical reason why $\omega(N)$ should remain finite. It is not an observable. What matters in a quantitative study of multiparticle correlation effects is the phase-space density of emission points and not the particle multiplicity, what matters are the weights v_m and u_m, and not the normalization $\omega(N)$.
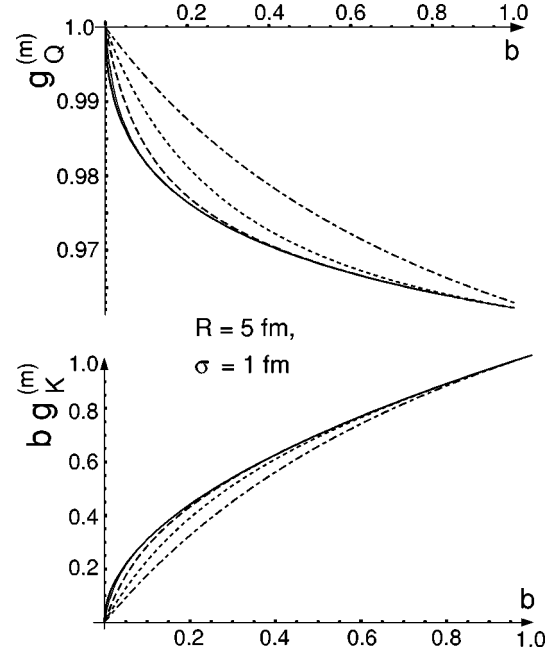

FIG. 2. Numerical calculation of the factors $g_Q^{(m)}$ and $bg_K^{(m)}$ which determine the $\mathbf{q}$ and $\mathbf{K}$ dependence of the mth order Pratt terms. For a source with spatial radius $R=5$ fm and a wave packet width $\sigma=1$ fm, the plot shows $g_Q^{(m)}$ and $bg_K^{(m)}$ as a function of $b = 1/(1+2/\sigma^2\Delta^2)$. Different lines denote different orders, $m=2$ (dash-dotted), $m=3$ (dotted), $m=5$ (dashed), $m=10$ (thin solid), and $m=100$ (solid).

We finally estimate realistic values for the phase-space density ρ_{vol} in heavy-ion collisions. For a choice of model parameters $R\approx5$ fm, $\sigma\approx1$ fm, $\Delta\approx150$ MeV say, we find $\epsilon\approx10^{-2}$. With multiplicities of like-sign pions in the hundreds, this leads to $\rho_{\mathrm{vol}}>1$. The present static, spherically symmetric model is however unrealistic in so far that it does not take the strong longitudinal expansion into account which significantly increases the volume out of which particles are emitted. From these heuristic considerations, we expect realistic phase-space densities to lie in the range

$$0.1 < \rho_{\mathrm{vol}} = \epsilon N < 1.0. \quad (4.16)$$

Depending on the precise value of ρ_{vol} in this range, the importance of multiparticle contributions to the one- and two-particle spectrum varies significantly. For $\rho_{\mathrm{vol}}=1.0$, higher-order contributions start dominating, while they account for $\approx10\%$ of the signal if $\rho_{\mathrm{vol}}=0.1$.

B. The momentum dependence of multiparticle contributions

The two m-dependent terms $g_K^{(m)}$ and $g_Q^{(m)}$ in Eq. (4.4) control the dependence of $G_m(\mathbf{P}_1,\mathbf{P}_2)$ on the relative pair momentum $\mathbf{q}$ and the average pair momentum $\mathbf{K}$. They determine the momentum dependence of all particle spectra. In Fig. 2, these factors are shown as a function of b for a source with $R=5$ fm and $\sigma=1$ fm. The first message of this plot is that even for very high multiparticle contributions (e.g., $m = 100$), the momentum dependence of all building blocks G_m can be calculated exactly. Secondly, the factors $g_Q^{(m)}$ and $bg_K^{(m)}$ show the interesting property that irrespective of the

value chosen for Δ (and hence for b), they rapidly converge to an m-independent quantity. In contrast to the limiting case (4.5a), the m dependence of $g_Q^{(m)}$ is much weaker for realistic model parameters a, b,

$$g_Q^{(m)} \rightarrow g_Q . \qquad (4.17)$$

Analogously, for realistic model parameters a, b,

$$b g_K^{(m)} \rightarrow b g_K , \qquad (4.18)$$

while for the limit (4.5b) of the parameter space, a strong m dependence remains.

We have checked that the conclusions (4.17), (4.18) hold for a large range of the model parameter space, including the part realistic for heavy-ion collisions. Going to smaller source sizes R (and hence to smaller values for a), the factor g_Q is found to deviate significantly from unity. Also, values for $b g_K$ vary significantly. The rapid convergence to the limiting behavior (4.17), (4.18) however is observed for all values $a > 0.1$. For choices of the model parameters realistic for heavy-ion collisions, the factors $b g_K^{(m)}$ and $g_Q^{(m)}$ are hence well approximated by an m-independent constant for sufficiently large m. We can write the higher-order Pratt terms as

$$G_m(\mathbf{P}_1, \mathbf{P}_2) = C_m f_g \exp[-A \mathbf{q}^2 - B \mathbf{K}^2], \qquad (4.19a)$$

$$f_g = \left(\frac{2\pi}{\Delta^2} b g_K \right)^{3/2}, \qquad (4.19b)$$

$$A = \left(\frac{\sigma^2}{4} + \frac{R^2}{8} \right) g_Q, \qquad (4.19c)$$

$$B = \frac{2b}{\Delta^2} g_K . \qquad (4.19d)$$

In Sec. IV D, we exploit this simple m dependence of the terms $g_K^{(m)}$, $g_Q^{(m)}$.

C. The one-particle spectrum

For the discussion of the one-particle spectrum, we introduce the temperature T via

$$\Delta^2 = 2MT. \qquad (4.20)$$

The model $\rho(\mathbf{p}, \mathbf{r})$ in Eq. (4.1) describes then a phase-space distribution of emission points with Boltzmann temperature T. Our aim is to determine how the slope and shape of the observed one-particle spectrum $\overline{\mathcal{P}}_N^1(\mathbf{P})$ changes with the slope T of this distribution $\rho(\mathbf{p}, \mathbf{r})$ and to what extent it is affected by multiparticle correlations. $\overline{\mathcal{P}}_N^1(\mathbf{P})$ is a superposition of Gaussians of different widths

$$\overline{\mathcal{P}}_N^1(\mathbf{P}) \propto \sum_{m=1}^{N} v_m e^{-E_{\mathbf{P}}/T_{\text{eff}}(m)}, \qquad (4.21a)$$
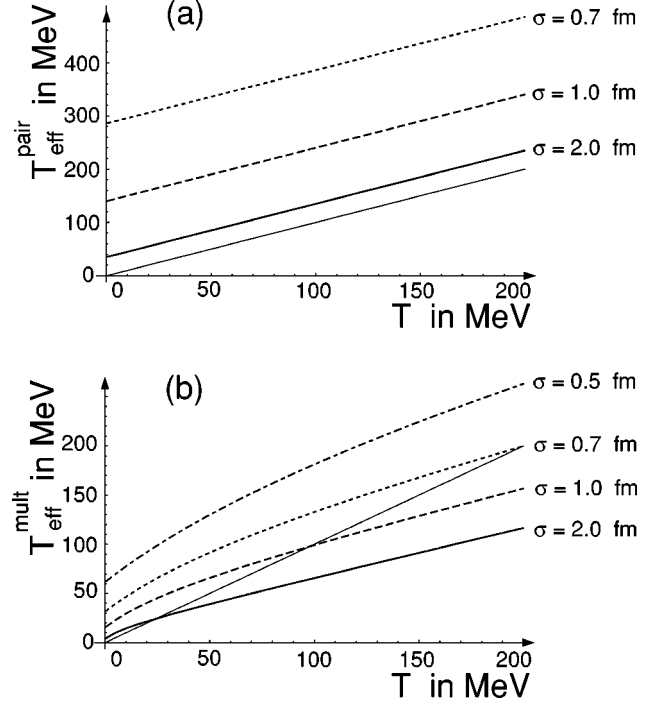

FIG. 3. The one-particle slope parameters $T_{\text{eff}}^{\text{pair}}$ and $T_{\text{eff}}^{\text{mult}}$ characterize the limiting cases of vanishing and dominant multiparticle correlation effects. They are shown as functions of the model temperature T for different values of the wave-packet width σ. The diagonals for $T_{\text{eff}} = T$ (thin solid lines) are included to guide the eye.

$$T_{\text{eff}}(1) = T_{\text{eff}}^{\text{pair}} = T + \frac{1}{2M\sigma^2}, \qquad (4.21b)$$

$$T_{\text{eff}}(m) = \frac{T}{2 b g_K^{(m)}} \quad m > 1 , \qquad (4.21c)$$

where $E_{\mathbf{P}} = \mathbf{P}^2/2M$, and $T_{\text{eff}}(m)$ characterizes the slope of the mth order contribution. According to Eq. (4.21), the one-particle spectrum cannot be characterized by a single slope parameter. For a qualitative understanding, we consider first the largest slope parameter $T_{\text{eff}}^{\text{pair}} = T_{\text{eff}}(1)$ and the smallest slope parameter $T_{\text{eff}}^{\text{mult}} = T_{\text{eff}}(m \gg 1)$. Here, the superscripts *pair* and *mult* stand for ''pairwise'' and ''multiparticle'' correlations.

If all multiparticle contributions vanish, then the momentum distribution of $\overline{\mathcal{P}}_N^1(\mathbf{P})$ coincides with that of $G_1(\mathbf{P}, \mathbf{P})$. The slope $T_{\text{eff}}^{\text{pair}}$ of $G_1(\mathbf{P}, \mathbf{P})$ is shown in Fig. 3(a) as a function of the model temperature T for the pion mass $M = 139$ MeV and different wave-packet localizations σ. $T_{\text{eff}}^{\text{pair}}$ is always larger than the model temperature T. For a spatial wave-packet width $\sigma = 1$ fm, e.g., the term $1/2M\sigma^2$ takes a value of 140 MeV. Even for small model temperatures T as input, the quantum contribution $1/2M\sigma^2$ accounts for a slope parameter $T_{\text{eff}}^{\text{pair}}$ comparable to the Hagedorn temperature. For this apparently leading effect, the notion ''quantum temperature'' was coined [15].

Figure 3(b) shows that multiparticle contributions can change this picture qualitatively, if they are dominant. The slope parameter $T_{\text{eff}}^{\text{mult}}$ still depends significantly on the choice of the wave-packet localization. But for model temperatures
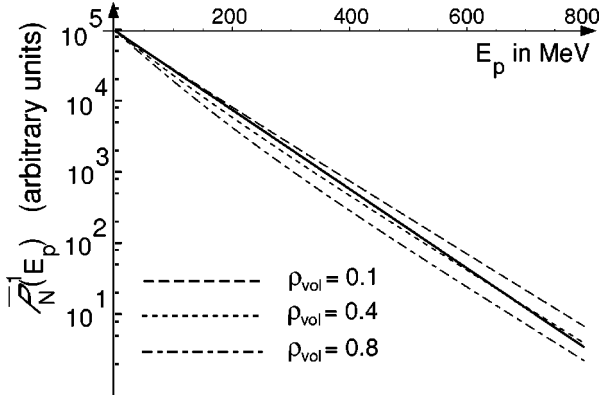
FIG. 4. The one-particle spectrum of a source typical for heavy-ion collisions ($R=5$ fm, $T=100$ MeV, $\sigma=1.2$ fm) becomes steeper with increasing phase-space density ρ_{vol} of emission points. The solid line characterizes a monoexponential behavior and is included for comparison.

in the range 100 MeV $<T<$ 200 MeV, there is always a value for σ, 0.7 fm $<\sigma<$ 1 fm, such that the observed temperature $T_{\mathrm{eff}}^{\mathrm{mult}}$ coincides with the model temperature T. For sufficiently large σ, the multiparticle effect can even overcompensate the broadening due to the quantum-mechanical localization, $T_{\mathrm{eff}}^{\mathrm{mult}}<T$. This illustrates that multiparticle symmetrization effects tend to populate the low momentum region of the one-particle spectrum, thereby increasing the slope of the spectrum. Both effects, this narrowing and the broadening due to the quantum-mechanical localization, are governed by the same scale σ and hence they cancel at least to some extent.

The lowest order term G_1 with slope parameter $T_{\mathrm{eff}}^{\mathrm{pair}}$ contributes a fraction $1/(1+\rho_{\mathrm{vol}})$ to the one-particle spectrum only. Hence, the one-particle spectrum $\bar{\mathcal{P}}_N^1$ is not monoexponential, but can be characterized by local slope parameters which specify the tangent onto $\bar{\mathcal{P}}_N^1$ at $E_{\mathbf{P}}=\mathbf{P}^2/2M$. Going to very large values of $E_{\mathbf{P}}$, the local slope always coincides with that of $T_{\mathrm{eff}}^{\mathrm{pair}}$, since the exponential of slowest decrease dominates in Eq. (4.21a). For sufficiently small $E_{\mathbf{P}}$ (below 2 GeV say), however, and for realistic phase-space densities, neither the pair nor the multiparticle contributions can be neglected. The local slope lies between $T_{\mathrm{eff}}^{\mathrm{pair}}$ and $T_{\mathrm{eff}}^{\mathrm{mult}}$. For a more quantitative statement, we have plotted in Fig. 4 the one-particle spectrum for different phase-space densities ρ_{vol} as a function of $E_{\mathbf{P}}$. Increasing ρ_{vol} and hence the contribution of multiparticle correlations, the local slope of the spectrum becomes steeper. Also, the superposition of Gaussians of different width leads to a slight curvature of the spectrum. Fitting the spectra in the range 0–1 GeV naively with a monoexponential thermal distribution, a variation of ρ_{vol} between 0 and 0.5 results in a change of the slope parameter

$$\Delta T_{\mathrm{eff}} \approx 20 \ \text{MeV}. \qquad (4.22)$$

This has to be taken properly into account in a quantitative analysis of hadron spectra.

We finally compare the spectrum (4.21a) to that of a Bose-Einstein distribution as obtained from an arbitrary initial phase-space distribution $\rho(\mathbf{p},\mathbf{r})$, keeping the bosons in a box till they have equilibrated,

$$\frac{1}{e^{(\mathbf{P}^2/2M-\mu)/T}-1} = \sum_{m=1}^{\infty} v_{\mathrm{BE}}^m e^{-m(\mathbf{P}^2/2M-\mu)/T}, \quad (4.23\mathrm{a})$$

$$v_{\mathrm{BE}}=e^{\mu/T}. \qquad (4.23\mathrm{b})$$

For the spectrum $\bar{\mathcal{P}}_N^1$ in Eq. (4.21) being of Bose-Einstein form, the weights v_m and the Pratt terms G_m would have to show a particular m dependence,

$$\mathrm{const} \cdot v_m = v_{\mathrm{BE}}{}^m, \qquad (4.24\mathrm{a})$$

$$G_m(\mathbf{P},\mathbf{P})/C_m = \exp[-mE_{\mathbf{P}}/T]. \qquad (4.24\mathrm{b})$$

In the present model, Eq. (4.24a) is satisfied by setting $v_{\mathrm{BE}} = \rho_{\mathrm{vol}}/(1+\rho_{\mathrm{vol}})$, see Eq. (4.11b). However, the m dependence of the terms $G_m(\mathbf{P},\mathbf{P})$ is in general weaker than what is required to match Eq. (4.24b). For the Zajc model, the m dependence of G_m is compatible with the Bose-Einstein distribution in the infinite volume limit. However, the Pratt terms C_m differ significantly from a power law which indicates a deviation from Eq. (4.24a). The reason for these differences is, that our model calculations of $\bar{\mathcal{P}}_N^1$ take a particular distribution $\rho(\mathbf{p},\mathbf{r})$ as initial condition and include Bose-Einstein symmetrization, but they do not contain an equilibration mechanism: the particles are emitted and propagate freely. Also, the N-particle state Ψ_N is not an equilibrium state. Hence, the spectrum $\bar{\mathcal{P}}_N^1$ depends in contrast to Eq. (4.23) on $\rho(\mathbf{p},\mathbf{r})$. In general, it is not a Bose-Einstein distribution.

D. The two-particle correlator

In this section, we first discuss the normalization of the two-particle correlator $C(\mathbf{K},\mathbf{q})$ and how it is calculated in the so-called pair approximation. Then we turn to the study of multiparticle effects.

1. Normalization of the two-particle correlator

There has been some debate recently about the appropriate normalization of the two-particle correlation function used in the HBT analysis of multiparticle production. For a compilation of the different normalizations used, and their problems, see Ref. [18]. In the present work, we use the normalization [2]

$$C(\mathbf{P}_1,\mathbf{P}_2) = \frac{\langle \hat{N} \rangle^2}{\langle \hat{N}(\hat{N}-1) \rangle} \frac{\sigma_\pi d^6 \sigma_{\pi\pi}/d^3\mathbf{P}_1 d^3\mathbf{P}_2}{(d^3\sigma_\pi/d^3\mathbf{P}_1)(d^3\sigma_\pi/d^3\mathbf{P}_2)}, \qquad (4.25)$$

where σ_π is the total pion cross section. This originates from normalizing both the single- and the double-differential cross sections to unity. Setting these cross sections proportional to the one- and two-particle spectra $\bar{\mathcal{P}}_N^1(\mathbf{P}_1)$, $\bar{\mathcal{P}}_N^2(\mathbf{P}_1,\mathbf{P}_2)$,

the two-particle correlator reads

$$C(\mathbf{P}_1,\mathbf{P}_2) = \frac{\bar{\mathcal{P}}_N^2(\mathbf{P}_1,\mathbf{P}_2)}{\bar{\mathcal{P}}_N^1(\mathbf{P}_1)\bar{\mathcal{P}}_N^1(\mathbf{P}_2)}. \tag{4.26}$$

The simplest way to make further progress is to assume that the approximation (4.19) for G_m is valid for all $m \geq 1$. Then, the two-particle spectrum can be written as

$$\bar{\mathcal{P}}_N^2(\mathbf{P}_1,\mathbf{P}_2) = \frac{\tilde{\omega}(N)}{\omega(N)} f_g e^{-A\mathbf{q}^2 - B\mathbf{K}^2},$$

$$\tilde{\omega}(N) = \sum_{J=2}^{N} \frac{(N-2)!}{(N-J)!} \omega(N-J) \sum_{i=1}^{J-1} C_i C_{J-i}, \tag{4.27}$$

and the correlator reads

$$C(\mathbf{P}_1,\mathbf{P}_2) = \frac{\tilde{\omega}(N)}{\omega(N)}\left(1 + \frac{e^{-2A\mathbf{q}^2 - 2B\mathbf{K}^2}}{e^{-B\mathbf{P}_1^2}e^{-B\mathbf{P}_2^2}}\right). \tag{4.28}$$

The normalization $\tilde{\omega}(N)/\omega(N)$ thus obtained in this approximation remains unchanged if the full m dependence of the Pratt terms G_m is included, though the momentum dependence of Eq. (4.28) is then much more involved.

The structure of the normalization $\tilde{\omega}(N)/\omega(N)$ is important for what follows: The term $\tilde{\omega}(N)$ contains exactly $N!/2$ terms, while $\omega(N)$ contains $N!$ terms. By integrating Eq. (2.10) over $\mathbf{P}_2$ and using the power-law behavior $C_m = \epsilon^{m-1}$, we find

$$\omega(N) - \tilde{\omega}(N) = \sum_{J=2}^{N} \frac{(N-2)!}{(N-J)!} \omega(N-J) \sum_{i=1}^{J-1} C_J, \tag{4.29a}$$

$$\frac{\tilde{\omega}(N)}{\omega(N)} = 1 - \epsilon. \tag{4.29b}$$

The normalization of the correlator is smaller than unity, the offset depends on the phase space volume occupied by the source. We shortly comment on the importance of this result:

The two-particle correlator can be viewed as the factor relating two-particle differential cross sections σ_{BE} of the real world (where Bose-Einstein symmetrization exists) to an idealized world in which Bose-Einstein correlations are absent,

$$\sigma_{\mathrm{BE}}(\mathbf{K},\mathbf{q}) = C(\mathbf{K},\mathbf{q})\sigma_{\mathrm{NO}}(\mathbf{K},\mathbf{q}). \tag{4.30}$$

If $C(\mathbf{K},\mathbf{q}) > 1$ everywhere, this implies that Bose-Einstein symmetrization effects increase the total cross section. For heavy-ion collisions, there is no direct test of whether such an enhancement exists. In e^+e^- collisions however, we know that Bose-Einstein correlations do not affect total cross sections appreciably, since, e.g., perturbative QCD predicts the production characteristics of Z_0 to a per mille level without invoking them. In our calculation, we start from an N-particle state and we require that after final state Bose-Einstein symmetrization, N particles are detected. Hence, we explicitly assume that final state Bose-Einstein correlations

do not affect the total cross sections. According to the above calculation, this automatically implies an offset of the normalization of $C(\mathbf{K},\mathbf{q})$ below unity. The offset ϵ in Eq. (4.29b) measures the system size from which particles are emitted. This is intrinsically consistent: for smaller system sizes (ϵ large), the correlator shows an enhancement in a broader $\mathbf{q}$ momentum region, and the normalization $(1-\epsilon)$ is smaller. This ensures that $\sigma_{\mathrm{BE}}^{\mathrm{tot}} = \sigma_{\mathrm{NO}}^{\mathrm{tot}}$.

We finally note that irrespective of the offset $\tilde{\omega}(N)/\omega(N)$ of the normalization, the correlator in Eq. (4.28) changes by a factor 2 between the limits $\mathbf{q}=0$ and $\mathbf{q}\to\infty$. This is a consequence of the approximation (4.19) which we have justified for the present model in Sec. IV B. In general, the $\mathbf{K}$ and $\mathbf{q}$ dependence of the Pratt terms G_m leads to a more complicated dependence of the correlator $C(\mathbf{K},\mathbf{q})$ according to Eq. (4.12). Depending on the model, this may affect the intercept of $C(\mathbf{K},\mathbf{q})$ at $\mathbf{q}=0$. Indeed, a decrease of the intercept with increasing event multiplicities was reported in recent model studies [4,10]. In contrast to the present study, these models however do not work with fixed event multiplicities and show a significantly different physics, including pion lasing effects [4]. We only conclude from the present study that multiparticle symmetrization effect do not lead automatically to a strong decrease of the intercept parameter.

2. The normalization in the pair approximation

We now explain why the offset $(1-\epsilon)$ of the normalization of $C(\mathbf{K},\mathbf{q})$ is not obtained in conventional calculations where multiparticle symmetrization effects are neglected. For the wave packets introduced in Sec. III, the wave-packet overlap functions f_{ij} in Eq. (3.4) shows a Gaussian decrease with the phase-space distance $|z_i - z_j|$. In general, the

$$\text{pair approximation: } f_{ij} = \delta_{ij} \tag{4.31}$$

is an uncontrolled approximation to this Gaussian behavior. It becomes exact in certain limiting cases

$$\lim_{\sigma\to 0} f_{ij} = \lim_{\sigma\to\infty} f_{ij} = \delta_{ij}. \tag{4.32}$$

In the pair approximation, all higher-order Pratt terms vanish

$$C_m = G_m(\mathbf{K},\mathbf{q}) = 0, \quad m \geq 2$$
$$\text{for } f_{ij} = \delta_{ij}, \tag{4.33}$$

and one regains the results of the conventional calculations where multiparticle effects are neglected: the two-particle correlator is normalized to unity,

$$\omega(N) = \tilde{\omega}(N) = 1 \quad \text{for } f_{ij} = \delta_{ij}. \tag{4.34}$$

and (2.6) does not change the phase space distribution since $\omega(N) = \langle \Psi_N | \Psi_N \rangle$. The term $G_1(\mathbf{P}_1,\mathbf{P}_2)G_1(\mathbf{P}_1,\mathbf{P}_2)$ in Eq. (4.12) then ensures that $C(\mathbf{P}_1,\mathbf{P}_2) > 1$. According to Eq. (4.30), this contradicts the statement $\sigma_{\mathrm{BE}}^{\mathrm{tot}} = \sigma_{\mathrm{NO}}^{\mathrm{tot}}$. The origin of this difficulty can be traced back to the integral

$$\int d^3\mathbf{P}_1 d^3\mathbf{P}_2 G_1(\mathbf{P}_1,\mathbf{P}_2)^2 = C_2, \tag{4.35}$$

which should vanish according to Eq. (4.33). The pair approximation does not treat the integral C_2 and the integrand of Eq. (4.35) on an equal footing. It sets $C_2 = 0$ but uses $G_1(\mathbf{P}_1,\mathbf{P}_2)^2$ for the calculation of the Bose-Einstein enhancement. It is this inconsistency which leads to a correlator $C(\mathbf{K},\mathbf{q}) > 1$ everywhere.

3. The HBT-radius parameters

Once the momentum-dependent higher-order Pratt terms G_m and their weights v_m, u_m are known, the determination of the two-particle correlator (4.26) is a matter of straightforward numerical calculation. From $C(\mathbf{K},\mathbf{q})$, the HBT-radius parameters are obtained by fitting the Gaussian ansatz

$$C(\mathbf{K},\mathbf{q}) \propto 1 + \lambda \exp[-R_{\mathrm{HBT}}^2 \mathbf{q}^2]. \tag{4.36}$$

We restrict our discussion to this one-dimensional parametrization of $C(\mathbf{K},\mathbf{q})$ since our model (4.1) is spherically symmetric. The general, analytical form of the two-particle correlator (4.26) is obtained from Eqs. (4.6) and (4.12) and it is quite involved. For a transparent discussion, we hence turn first to limiting cases. In the pair approximation, when all multiparticle effects are neglected, we obtain from Eq. (4.2b) the well-known result [11]

$$R_{\mathrm{HBT}}^{\mathrm{pair}\,2} = \frac{R^2}{2} + \frac{\sigma^2}{2}\frac{\Delta^2\sigma^2}{1+\Delta^2\sigma^2}. \tag{4.37}$$

The other, equally unrealistic limiting case is that multiparticle contributions dominate completely. The resulting two-particle correlator is given in Eq. (4.28) and the corresponding HBT-radius parameter reads

$$R_{\mathrm{HBT}}^{\mathrm{mult}\,2} = \frac{R^2}{4} g_Q + \frac{\sigma^2}{2}\frac{g_Q\sigma^2\Delta^2 + 2g_Q - g_K}{\sigma^2\Delta^2 + 2}. \tag{4.38}$$

The difference between these two expressions is significant. For a discussion of the main qualitative and quantitative effects, we now focus on the parameter region $R^2 \gg \sigma^2$ relevant for relativistic heavy-ion collisions. In this regime, the $\sigma^2/2$-dependent parts of Eqs. (4.37) and (4.38) can be neglected, and according to the study of Sec. IV B, $g_Q \approx 1$. We then find the simple relation

$$R_{\mathrm{HBT}}^{\mathrm{mult}} \approx \frac{1}{\sqrt{2}} R_{\mathrm{HBT}}^{\mathrm{pair}}, \quad \text{for } R \gg \sigma. \tag{4.39}$$

This is the factor 2, obtained first by Zajc [3] in his comparison of the first- and second-order Pratt terms, see Eq. (2.17). Zajc has given an estimate that in his model, multiparticle effects change the HBT radius parameter by as much as a factor 0.67 for a particle density of 1 per unit phase-space cell [3]. This would affect estimates of the source volume or the energy density by a factor 3. In Zajc's model, however, higher-order multiparticle effects ($m > 2$) change the $\mathbf{q}$ dependence of $C(\mathbf{K},\mathbf{q})$ much more dramatically than in the present study, where $g_Q^{(m)}$ has a very weak m dependence, negligible for $R^2 \gg \sigma^2$.

In our model, the correlator is a weighted superposition of Gaussians in $\mathbf{q}$ whose widths differ by as much as a factor
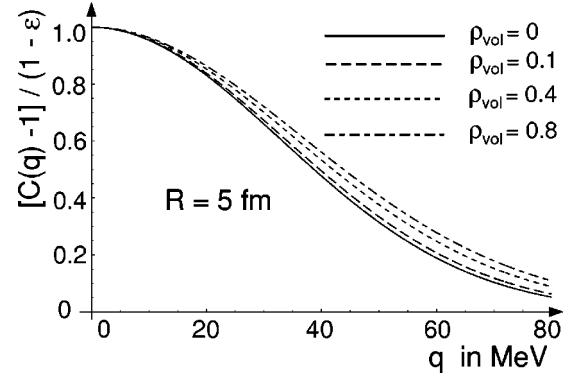

FIG. 5. Multiparticle symmetrization effects broaden the two-particle correlator. For a source size of $R = 5$ fm, the plot shows the resulting two-particle correlator for different particle phase space densities ρ_{vol}.

$\sqrt{2}$. In Fig. 5, we have plotted the resulting two-particle correlator for relatively low phase-space densities where the lowest-order Pratt term G_1 is still the leading contribution. The result of the pair approximation describes the main behavior, but deviations due to multiparticle contributions affect the HBT-radius parameter on a 10% level for moderate phase-space densities. This 10% effect translates into underestimating the volume by 30% and overestimating the corresponding energy density by a similar amount. In models which show a stronger m dependence of the momentum-dependent part of G_m, the effect may be significantly stronger. In general, the degree to which multiparticle effects modify HBT radius parameters depends significantly on the phase-space density of emission points.

V. MULTIPARTICLE CORRELATIONS FOR ARBITRARY MODELS

In this section, we shortly discuss how the calculation of multiparticle correlation effects can be extended to more realistic source distributions where the analytical techniques used in Sec. IV are not applicable. Pratt has shown already how to calculate the terms C_m and $G_m(\mathbf{P}_1,\mathbf{P}_2)$ for *continuous* source functions [4]: up to order $m \le 5$, straightforward Monte Carlo methods can be used, and an improved Metropolis method allows to push numerical calculations up to $m \approx 20$. This seems to be sufficient for all practical purposes, since according to our model study, the weights v_m, u_m for $m > 20$ are negligible for realistic phase-space densities ρ_{vol}.

Here, we propose yet a different technique which is applicable to events characterized by a set of N *discrete* phase space points $(\mathbf{p}_i,\mathbf{r}_i,t_i)$. We interpret these points as the centers of Gaussian single-particle wave packets, i.e.,

$$(\mathbf{p}_i,\mathbf{r}_i,t_i) \to f_i. \tag{5.1}$$

An arbitrary distribution of N discrete phase-space points is the most general "source model" in the present framework. We first discuss algorithms which allow for the calculation of the two-particle correlator from a set $(\mathbf{p}_i,\mathbf{r}_i,t_i)$. Then we comment on applications of these algorithms to event generators.

A. An algorithm for Bose-Einstein weights

We start with the simplest case, the pair approximation, which reduces the sum over $N!$ terms in the two-particle spectrum to a sum over all $\frac{1}{2}N(N-1)$ particle pairs (i,j). Each pair is weighted with the pair probability $\mathcal{P}_{ij}$, calculated from the corresponding two-particle symmetrized state [11].

$$\mathcal{P}_{ij}(\mathbf{P}_1,\mathbf{P}_2)=\frac{1}{2}|D_i(\mathbf{P}_1)D_j(\mathbf{P}_2)+D_i(\mathbf{P}_2)D_j(\mathbf{P}_1)|^2,\tag{5.2}$$

$$\mathcal{P}_N^2(\mathbf{P}_1,\mathbf{P}_2)=\frac{2}{N(N-1)}\sum_{(i,j)}\mathcal{P}_{ij}(\mathbf{P}_1,\mathbf{P}_2).$$

To compare this expression to the ZP algorithm, we introduce the quantities

$$G_1(\mathbf{P}_1,\mathbf{P}_2)=\frac{1}{N}\sum_{i=1}^N D_i^*(\mathbf{P}_1)D_i(\mathbf{P}_2),\tag{5.3a}$$

$$T_c(\mathbf{P}_1,\mathbf{P}_2)=\frac{1}{N^2}\sum_{i=1}^N D_i^*(\mathbf{P}_1)D_i(\mathbf{P}_1)D_i^*(\mathbf{P}_2)D_i(\mathbf{P}_2).\tag{5.3b}$$

Here, $G_1(\mathbf{P}_1,\mathbf{P}_2)$ is the first-order Pratt term for the discrete phase-space distribution $(\mathbf{p}_i,\mathbf{r}_i,t_i)$ and T_c is a finite multiplicity correction, correcting for the double counting of identical pairs (i,i) in

$$\sum_{(i,j)}\mathcal{P}_{ij}(\mathbf{P}_1,\mathbf{P}_2)=G_1(\mathbf{P}_1,\mathbf{P}_2)G_1(\mathbf{P}_1,\mathbf{P}_2)$$
$$+G_1(\mathbf{P}_1,\mathbf{P}_2)G_1(\mathbf{P}_1,\mathbf{P}_2)-2T_c(\mathbf{P}_1,\mathbf{P}_2).\tag{5.4}$$

In the large multiplicity limit, when T_c can be neglected, this expression is equivalent to the pair approximation of the ZP algorithm, see, e.g. Eq. (4.12a). The one-particle spectrum ν and the two-particle correlation obtained in this way have been discussed already extensively in [11]. They can be rewritten in terms of the single-particle probabilities s_i of Eq. (3.3b),

$$C(\mathbf{K},\mathbf{q})=1+\frac{e^{-\sigma^2\mathbf{q}^2/2}|\Sigma_{i=1}^N s_i(\mathbf{K})e^{i\mathbf{r}_i\cdot\mathbf{q}}|^2-T_c}{\nu(\mathbf{P}_1)\nu(\mathbf{P}_2)-T_c},\tag{5.5a}$$

$$\nu(\mathbf{P})=\sum_{i=1}^N s_i(\mathbf{P}),$$

$$T_c(\mathbf{P}_1,\mathbf{P}_2)=\sum_{i=1}^N s_i(\mathbf{P}_1)s_i(\mathbf{P}_2).\tag{5.5b}$$

The number of numerical operations needed to calculate this correlator grows linearly with the multiplicity N rather than quadratic as in Eq. (5.2) and this makes it particularly suitable for a numerical algorithm. At given observed momenta $\mathbf{K}$, $\mathbf{q}$, one calculates for each event the one-particle probabilities $s_i(\mathbf{K})$ according to Eq. (3.3b) and performs the sums in Eq. (5.5). The $s_i(\mathbf{K})$ are continuous in the measured momen-

tum, and hence the obtained correlator is a continuous function of $\mathbf{K}$ and $\mathbf{q}$, i.e., no binning is required. At high multiplicities, when the factors T_c are negligible, the correlator (5.5) can be rewritten as a Fourier transform over an emission function $S(x,\mathbf{K})$, thereby regaining the well-known starting point of most model studies, (see Refs. [11],[16] for further details)

$$C(\mathbf{K},\mathbf{q})=1+\frac{|\int d^4x S(x,\mathbf{K})e^{ix\cdot q}|^2}{\int d^4x S(x,\mathbf{P}_1)\int d^4y S(y,\mathbf{P}_2)},\tag{5.6a}$$

$$S(x,K)=\sum_{i=1}^\infty S_i(x,\mathbf{K}),\tag{5.6b}$$

$$S_i(x,\mathbf{K})\propto\delta(t-t_i)e^{-1/\sigma^2(\mathbf{x}-\mathbf{r}_i)^2-\sigma^2(\mathbf{K}-\mathbf{p}_i)^2}.$$

The above discussion shows that in the pair approximation, a numerical algorithm for the calculation of one- and two-particle spectra can be based on a discrete version of the first-order Pratt terms G_1. Here, we propose to extend this approach to take multiparticle correlations into account by calculating

$$C_m=\frac{(N-m)!}{N!}\sum_{i_1\ldots i_m}f_{i_1 i_2}\ldots f_{i_{m-1}i_m}f_{i_m i_1},\tag{5.7a}$$

$$G_m(\mathbf{P}_1,\mathbf{P}_2)$$
$$=\frac{(N-m)!}{N!}\sum_{i_1\ldots i_m}D_{i_1}^*(\mathbf{P}_1)f_{i_1 i_2}\ldots f_{i_{m-1}i_m}D_{i_m}(\mathbf{P}_2).\tag{5.7b}$$

The sums in these expressions run over all sets of m out of N integers and over all $m!$ permutations of each set. This implies that for event multiplicities in the hundreds, only terms up to order $m\approx 5$ can be calculated in a reasonable amount of CPU time. A tentative strategy for calculating multiparticle correlation effects on the basis of Eq. (5.7) then proceeds as follows:

(1) Fit the calculated terms C_m to a power law $C_m=\epsilon^{m-1}$ and use the parameter ϵ thus determined for a calculation of the weights v_m, u_m in Eqs. (4.6) and (4.12a).
(2) Fit Gaussians in $\mathbf{K}$ and $\mathbf{q}$ to the momentum-dependent Pratt terms $G_m(\mathbf{P}_1,\mathbf{P}_2)$. This allows us to extract the terms $g_K^{(m)}$ and $g_Q^{(m)}$ which govern the momentum dependence of multiparticle effects.
(3) Calculate the one- and two-particle spectra by including up to the numerically determined order, $m=5$ say, all contributions exactly, approximating the momentum dependence of higher-order terms by setting $g_K^{(m)}=g_K^{(5)}$, $g_Q^{(m)}=g_Q^{(5)}$ for $m>5$.

This scheme draws on the experience gained from the study of the Gaussian toy model in Sec. IV. We expect that it allows to estimate multiparticle contributions for model distributions $(\mathbf{p}_i,\mathbf{r}_i,t_i)$.

B. Bose-Einstein weights for event generators

Many event generators for the simulation of heavy-ion collisions have been developed in recent years [19–23], and irrespective of the large variety of physical inputs present in their codes, the typical output of their event simulation contains for each event a set Σ of N phase space points $(\mathbf{p}_i, \mathbf{r}_i, t_i)$ which one associates with the final-state particles produced. However, a choice of interpretation is involved in comparing an event generator output $z_i = (\mathbf{p}_i, \mathbf{r}_i, t_i)$ to experimental data. Usually, the measured one-particle spectra are compared directly to the binned momenta $\mathbf{p}_i$, i.e., one implicitly interprets the simulated phase-space points z_i as defining momentum eigenstates, which a fortiori carry no space-time information. For the calculation of two-particle correlations, this interpretation is not suitable, it leads to a sharp δ-like correlator [11]. Also, a classical interpretation of z_i which takes both $\mathbf{r}_i$ and $\mathbf{p}_i$ as ''sharp'' information, is problematic: ignoring the correct quantum-mechanical localization leads to quantitatively and qualitatively unreliable results [24]. On the other hand, including a quantum-mechanical localization width σ, one changes both the one- and two-particle spectrum by a prescription which has no dynamical foundation.

The origin of these difficulties in finding a consistent interpretation of the event generator output $z_i = (\mathbf{p}_i, \mathbf{r}_i, t_i)$ is well known, see, e.g., Refs. [25],[26]: quantum-mechanical processes require a description in terms of amplitudes, while event simulations are formulated in a probabilistic setting. Bose-Einstein correlations occur by symmetrizing the production amplitudes of identical particles and are hence not encoded for in event generators. The mere fact that the simulated output is a discrete phase-space distribution of emission points without identical multiparticle correlations (rather than a set of detected momenta which includes all multiparticle correlations and hence all space-time information available from the measurement), is the very consequence of using a probabilistic language. In practice, this forces one to take recourse to an algorithm which associates a posteriori Bose-Einstein weights with the simulated phase-space distribution Σ, rather than obtaining these correlations from the dynamical propagation of properly (anti)-symmetrized N-particle states. This a posteriori modification of an incomplete quantum-dynamical evolution creates the interpretational problems of the output $z_i = (\mathbf{p}_i, \mathbf{r}_i, t_i)$. Phenomenologically motivated numerical simulations of heavy-ion collisions have remarkable success despite these fundamental problems. It is of some interest to confront them with experimental two-particle correlations, since this provides a test of their spatiotemporal (rather than only their momentum-dependent) properties. We expect that the algorithms discussed in Sec. V A are useful in such comparisons.

VI. CONCLUSION

The Zajc-Pratt algorithm provides a simple technique for the calculation of multiparticle symmetrization effects in one- and two-particle spectra. Based on this algorithm, we have studied to what extent multiparticle correlations steepen the slope of the one-particle and broaden the width of the two-particle spectrum. The scale of both effects depends sensitively on the particle phase-space density ρ_{vol} in the emission region. Multiparticle correlations contribute a fraction $\rho_{\mathrm{vol}}/(1+\rho_{\mathrm{vol}})$ to the one-particle spectrum and a fraction $1 - 1/(1+\rho_{\mathrm{vol}})^2$ to the two-particle spectrum. Also, the m dependence of higher-order Pratt terms, i.e., the extent to which the momentum dependence of multiparticle contributions G_m changes with increasing order m, plays an important role. In a Gaussian source model with instantaneous emission and moderate particle phase-space densities, the slope parameter T_{eff} of the one-particle spectrum changes by up to 20 MeV, and the change in the HBT radius parameters is of the order of 10%, if multiparticle effects are neglected.

For the reconstruction program advocated in [1], our results indicate that neglecting multiparticle effects, one underestimates the source temperature significantly and one overestimates the energy density by up to 30%. Here, the caveat is however that our calculation does not include multiparticle final-state Coulomb interactions. Bose-Einstein and Coulomb effects typically arise on the same scale and compensate each other at least to some extent. This may significantly reduce the effect of multiparticle correlations in the measured π^+ and π^- spectra on which most of the phenomenological analysis is based currently. It will hence be very interesting to compare the slopes of the one-particle spectra of charged and neutral pions [27]. On the basis of the above heuristic ideas, one may expect the slope of the π^0 spectrum to be somewhat steeper, since multiparticle Coulomb interactions cannot compensate for the multiparticle Bose-Einstein symmetrization effects.

Our analysis of multiparticle effects has also shed new light on a recent discussion about the normalization of the two-particle correlator. Defining the correlator via Eq. (4.25), it is normalized for large relative momenta $\mathbf{q}$ to $(1-\epsilon)$, and not to unity. The importance of this result was already discussed in Sec. IV D 1: the normalization (4.29b) corrects the result of the commonly used pair approximation and leads to Bose-Einstein unit weights which conserve event probabilities.

We close by embedding the present work into a wider perspective: Many aspects of the dynamical evolution of relativistic heavy-ion collisions are mesoscopic, and this makes it very difficult to decide whether certain physical observables have a known conventional interpretation or are indicative of the new in-medium properties which the current experimental programs at CERN and RHIC aim for. The physics of final-state hadrons however, though being mesoscopic and hence difficult to treat, is known in principle. It allows hence for a detailed quantitative description on the basis of present day knowledge. In a second step, such a description will pave the way for quantitative statements about the geometry and dynamics of the final stage of the collision process, thereby setting up an experimentally motivated starting point for a dynamical back extrapolation [1]. We hope that the present work, by quantifying one mesoscopic multiparticle effect, will prove useful in refining this reconstruction program and in separating known physics from the in-medium properties we are looking for.
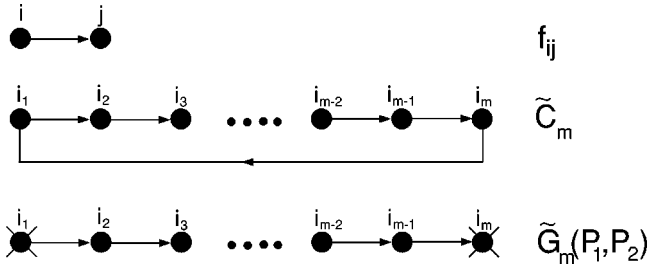
FIG. 6. Diagrammatic representation of the types of factors contributing to multiparticle spectra.

APPENDIX A: DERIVATION OF THE ZP ALGORITHM

So far, there is no self-contained derivation of the Zajc-Pratt algorithm in the literature. For the convenience of the reader, we give here the main arguments.

Notation: We denote the term $f_{i_1 i_2}$ by an arrow from i_1 to i_2. m of these terms form a closed m cycle $\tilde{C}_m$. The only other structure appearing in all spectra are open m cycles $\tilde{G}_m$, see Fig. 6. Here, $D^*_{i_1}$ is represented by a cross from which the arrow starts, D_{i_1} by a cross at which the arrow ends. The Pratt terms C_m, G_m are obtained by averaging the emission points in Fig. 6 over a model distribution $\rho(\mathbf{p},\mathbf{r},t)$. Dots without indices attached indicate that this average was carried out, see Fig. 7.

Normalization: The normalization $w(N)=\bar{\mathcal{P}}^0_N$ sums the products $C_1^{l_1} C_2^{l_2} \dots C_n^{i_n}$ over all partitions $(n,l_n)_N$. Each partition of $(n,l_n)_N$ has $N!/\prod_n n!^{l_n}(l_n!)$ possible realizations. These have to be multiplied by the $(n-1)!$ different ways to combine each set of n points to a closed cycle. This leads to the prefactor $N!/\prod_n n^{l_n}(l_n!)$ in Eq. (2.8).

There exists a simple diagrammatic prescription to construct from the terms of $w(N)$ the terms of $w(N+1)$. One adds to each diagram of $w(N)$ an $(N+1)$th dot by

FIG. 7. Diagrammatic representation of the averaged total multiplicity $w(N)$. The 2 cycle stands for C_2, the 3 cycle for C_3, etc.

FIG. 8. Diagrammatic representation of the one-particle spectrum for multiplicities $N=1,2,3$.

(1) placing the dot once disconnected from all other cycles.

(2) changing closed m cycles C_m into m closed $(m+1)$ cycles C_{m+1}.
This prescription can be checked, e.g., in Fig. 7. It automatically insures, that $w(N)$ is represented by $N!$ diagrams, the maximal value for $w(N)$ is $N!$.

One-particle spectrum: Each term of $\omega(N)\bar{\mathcal{P}}^1_N(\mathbf{P})$ has the structure $w(N-m)G_m$: it contains exactly one open m cycle $G_m(P,P)$, the $N-m$ other dots being contained in closed cycles. To construct from it the terms of $\omega(N+1)\bar{\mathcal{P}}^1_{N+1}(\mathbf{P})$ one has to use the replacement

$$w(N-m)G_m \to w(N+1-m)G_m + w(N-m)mG_{m+1}. \tag{A1}$$

Diagrammatically, this is realized by employing the two diagrammatic rules given above and supplementing them with

(3) change open m cycles G_m into m open $(m+1)$ cycles G_{m+1}.
The prescription can be checked, e.g., in Fig. 8. Using the recursion relation (A1), one can prove by complete induction that the averaged one-particle spectrum $\bar{\mathcal{P}}^1_N(\mathbf{P})$ takes the form (2.9).

Two-particle spectrum: In $\omega(N)\bar{\mathcal{P}}^2_N(\mathbf{P_1},\mathbf{P_2})$, each term contains two open cycles of lengths i and j, the $N-i-j$ remaining dots being contained in closed cycles, divided by the normalization $\omega(N)$. On the endpoints of the two open cycles G_i and G_j, the momenta $\mathbf{P_1}$ and $\mathbf{P_2}$ can be attached in different combinations: for $i=j$, there are two possibilities, for $i \neq j$, there are four. This combinatorics is properly encoded in the definition of the product $G_{i,j} = C_i C_j H_{i,j}/(1 + \delta_{ij})$, see Eq. (4.12b). An $N \to (N+1)$ recursion relation for the two-particle spectrum is obtained by using the rule to change open m cycles into m open $(m+1)$ cycles, and properly treating the combinatorics for $i=j$,

$$w(N-i-j)G_{i,j} \to w(N-i-j)[i(1+\delta_{i+1,j}-\delta_{i,j})G_{i+1,j}$$
$$+jG_{i,j+1}]+w(N+1-i-j)G_{i,j}. \tag{A2}$$

Expression (2.10) for the two-particle spectrum then follows from Eq. (A2) by complete induction.

APPENDIX B: CALCULATION OF MULTIPARTICLE EFFECTS

Here, we give details of the calculation of higher-order Pratt terms C_m and G_m for the Gaussian source model (4.1)

in Sec. IV. Due to the structure of the functions f_{ij}, it is advantageous to change to relative and average momentum variables. For an average over m phase-space points, we introduce the integration variables

$$a_i = p_i - p_{i+1}, \quad b_i = r_i - r_{i+1}, \quad \text{for } i \in [1, m-1],$$
(B1a)

$$a_m = p_m + p_1, \quad b_m = r_m + r_1.$$
(B1b)

In terms of these variables, the building blocks for the mth order Pratt terms read

$$f_{12}f_{23} \cdots f_{(m-1)m} = \prod_{j=1}^{m-1} e^{-(\sigma^2/4) a_j^2 - (1/4\sigma^2) b_j^2 + ib_j A_j},$$
(B2a)

$$A_n = -\frac{1}{2}\sum_{j=1}^{n-1} a_j + \frac{1}{2}\sum_{j=n+1}^{m-1} a_j,$$
(B2b)

$$f_{m1} = e^{-(\sigma^2/4)\left(\sum_{j=1}^{m-1} a_j\right)^2 - 1/4\sigma^2\left(\sum_{j=1}^{m-1} b_j\right)^2} e^{-(i/2) a_m \sum_{j=1}^{m-1} b_j},$$
(B2c)

$$D_1(\mathbf{P}_1)D_m^*(\mathbf{P}_2) = e^{-\sigma^2(a_m/2 - \mathbf{K})^2 - i\mathbf{K}\sum_{j=1}^{m-1} b_j}$$
$$\times e^{-(\sigma^2/4)\left(\mathbf{q} + \sum_{j=1}^{m-1} a_j\right)^2 + i\mathbf{q}(b_m/2)}.$$
(B2d)

For the Gaussian emission probability (4.1), the probability ρ_2 of having two particles with wave packets centered around phase-space points $(\mathbf{r}_i, \mathbf{p}_i)$, $(\mathbf{r}_j, \mathbf{p}_j)$, is given by the product $\rho(\mathbf{r}_i, \mathbf{p}_i) \cdot \rho(\mathbf{r}_j, \mathbf{p}_j)$ and factorizes into a probability distribution for the relative and average particle pair coordinates,

$$\rho_2(\mathbf{p}_i, \mathbf{p}_j, \mathbf{r}_i, \mathbf{r}_j) = \rho(\mathbf{p}_i, \mathbf{r}_i)\rho(\mathbf{p}_j, \mathbf{r}_j)$$
$$= \rho_{\text{rel}}(\mathbf{p}_i - \mathbf{p}_j, \mathbf{r}_i - \mathbf{r}_j)\rho_{\text{ave}}(\mathbf{p}_i + \mathbf{p}_j, \mathbf{r}_i + \mathbf{r}_j),$$
(B3a)

$$\bar{\rho}(a,b) = \rho_{\text{rel}}(a,b) = \rho_{\text{ave}}(a,b)$$
$$= \frac{1}{(2\pi)^3 R^3 \Delta^3} e^{-(a^2/2\Delta^2) - (b^2/2R^2)}.$$
(B3b)

We then define the higher-order Pratt terms as averages over pair distribution probabilities

$$G_m(\mathbf{P}_1, \mathbf{P}_2) = \int \left(\prod_{j=1}^{m} d^3 a_j d^3 b_j \bar{\rho}(a_j, b_j)\right)$$
$$\times D_1(\mathbf{P}_1)f_{12}f_{23}\cdots f_{(m-1)m}D_m^*(\mathbf{P}_2).$$
(B4)

This is a Gaussian integral which can be calculated analytically. Its exponent is diagonal in all integration variables b_i and in a_m, and doing the corresponding integrals leads to

$$G_m(\mathbf{P}_1, \mathbf{P}_2) = \left(\left[1 + \frac{\sigma^2 \Delta^2}{2}\right]\left[1 + \frac{R^2}{2\sigma^2}\right]\right)^{-3(m-1)/2} \gamma^{-3/2}$$
$$\times e^{-\sigma^2/4 (1 + R^2/2\sigma^2)\mathbf{q}^2} e^{-2/\Delta^2 (1 - 1/\gamma)\mathbf{K}^2}$$
$$\times I(\mathbf{K}, \mathbf{q}),$$
(B5a)

$$\gamma = \frac{1}{1-b}[1 + ab(m-1)].$$
(B5b)

Here, the notational shorthands a, b of Eq. (4.3d) are used again,

$$I(\mathbf{K}, \mathbf{q}) = \pi^{-3(m-1)/2} \int \left(\prod_{j=1}^{m-1} d^3 a_j\right)$$
$$\times \exp[-a_i \mathbf{M}_{ij} a_j + (w_i + v_i)r_i],$$
(B6a)

$$w_i = \mathbf{q}\sigma\sqrt{b},$$
(B6b)

$$v_i = \mathbf{K}2\sigma\sqrt{b}a(2i-m)/\gamma,$$
(B6c)

$$\mathbf{M}_{ij} = \delta_{ij} + b + ab(m - 1 - 2|i-j| - \delta_{ij})$$
$$- \frac{a^2 b^2}{ab(m-1)+1}(2i-m)(2j-m).$$
(B6d)

The integral $I(\mathbf{K}, \mathbf{q})$ can be calculated explicitly [13],

$$\det \mathbf{M} = \frac{h_2^{(m)} h_3^{(m)}}{1 + ab(m-1)},$$
(B7a)

$$\frac{1}{4}v_i \mathbf{M}_{ij}^{-1} w_j = 0,$$
(B7b)

$$\frac{1}{4}v_i \mathbf{M}_{ij}^{-1} v_j = 2\frac{(\gamma - 1)h_3^{(m)} - b\gamma h_1^{(m)}}{\Delta^2 \gamma h_3^{(m)}}\mathbf{K}^2,$$
(B7c)

$$\frac{1}{4}w_i \mathbf{M}_{ij}^{-1} w_j = \frac{\sigma^2}{4}\frac{1}{1-a}\frac{h_2^{(m)} - h_3^{(m)}}{h_2^{(m)}}\mathbf{q}^2.$$
(B7d)

The factors $h_1^{(m)}$, $h_2^{(m)}$, and $h_3^{(m)}$ are defined in Eqs. (4.3) and (4.4).

[1] U. Heinz, in Proceedings of the XXVth Int. Workshop on Gross Properties of Nuclei and Nuclear Excitations, Hirschegg, Austria, 1997, nucl-th/9701054; U. A. Wiedemann in Proc. of the XXXIInd Rencontres de Moriond, Les Arcs, France, 1997, nucl-th/9705042; U. A. Wiedemann, talk at the 13th Int. Conf. on Ultra-relativistic Nucleus-Nucleus Collisions (Quark Matter'97), Tsukuba, Japan, 1997 [Nucl. Phys. A (in press)], nucl-th/9801017.

[2] M. Gyulassy, S. K. Kauffmann, and L. W. Wilson, Phys. Rev. C **20**, 2267 (1979).

[3] W. A. Zajc, Phys. Rev. D **35**, 3396 (1987); W. A. Zajc *et al.*, Phys. Rev. C **29**, 2173 (1984).

[4] S. Pratt, Phys. Lett. B **301**, 159 (1993); Phys. Rev. C **50**, 469 (1994); S. Pratt and V. Zelevinsky, Phys. Rev. Lett. **72**, 816 (1994).

[5] W. N. Zhang *et al.*, Phys. Rev. C **47**, 795 (1993).

[6] A. Bialas and A. Krzywicki, Phys. Lett. B **354**, 134 (1995).

[7] N. Amelin and R. Lednicky, Heavy Ion Physics **4**, 241 (1996).

[8] K. Fialkowski and R. Wit, hep-ph/9703227; hep-ph/9709205; Acta Phys. Pol. B **28**, 2039 (1997).

[9] J. Wosiek, Phys. Lett. B **399**, 130 (1997).

[10] T. Csörgö and J. Zimányi, Phys. Rev. Lett. **80**, 916 (1998); J. Zimányi and T. Csörgö, hep-ph/9705432.

[11] U. A. Wiedemann, P. Foka, H. Kalechofsky, M. Martin, C. Slotta, and Q. H. Zhang, Phys. Rev. C **56**, R614 (1997).

[12] M. Hillery, R. F. O'Conell, M. Scully, and E. P. Wigner, Phys. Rep. **106**, 121 (1984).

[13] S. Wolfram, The MATHEMATICA Book, 3rd ed. (Cambridge University Press, Cambridge, 1996).

[14] S. Padula, M. Gyulassy, and S. Gavin, Nucl. Phys. **B329**, 357 (1990).

[15] H. Merlitz and D. Pelte, Z. Phys. A **357**, 175 (1997).

[16] Q. H. Zhang, U. A. Wiedemann, C. Slotta, and U. Heinz, Phys. Lett. B **407**, 33 (1997).

[17] I. S. Gradshteyn and I. M. Ryzhik, *Table of Integrals, Series and Products* (Academic, New York, 1980).

[18] D. Miśkowiec and S. Voloshin, nucl-ex/9704006.

[19] H. Sorge, H. Stöcker, and W. Greiner, Ann. Phys. (N.Y.) **192**, 266 (1989).

[20] K. Werner, Phys. Rep. **232**, 87 (1993).

[21] Y. Pang, T. J. Schlagel, and S. H. Kahana, Phys. Rev. Lett. **68**, 2743 (1992); T. J. Schlagel, Y. Pang, and S. H. Kahana, *ibid.* **69**, 3290 (1992).

[22] K. Geiger, Comput. Phys. Commun. **104**, 70 (1997).

[23] X. N. Wang and M. Gyulassy, Phys. Rev. D **44**, 3501 (1991); Comput. Phys. Commun. **83**, 307 (1994).

[24] M. Martin, H. Kalechofsky, P. Foka, and U. A. Wiedemann, Eur. Phys. J. C **2**, 359 (1998).

[25] L. Lönnblad and T. Sjöstrand, Phys. Lett. B **351**, 293 (1995); Eur. Phys. J. C **2**, 165 (1998) .

[26] J. Aichelin, Nucl. Phys. **A617**, 510 (1997).

[27] T. Peitzmann for the WA98 Collaboration, talk at the 13th Int. Conf. on Ultra-relativistic Nucleus-Nucleus Collisions (Quark Matter'97), Tsukuba, Japan, 1997 [Nucl. Phys. A (in press)].